Available online at www.sciencedirect.com
SCIENCE DIRECT®
Journal of Catalysis 236 (2005) 356–365
JOURNAL OF CATALYSIS
www.elsevier.com/locate/jcat

Partially reduced heteropolyanions for the oxidative dehydrogenation of ethane to ethylene and acetic acid at atmospheric pressure

J.M. Galownia [a], A.P. Wight [a,1], A. Blanc [a,2], J.A. Labinger [b], M.E. Davis [a,*]

[a] *Chemical Engineering, California Institute of Technology, Pasadena, CA 91125, USA*
[b] *Beckman Institute, California Institute of Technology, Pasadena, CA 91125, USA*

Received 3 August 2005; revised 11 October 2005; accepted 12 October 2005

Available online 11 November 2005

Abstract

Niobium- and pyridine-exchanged salts of phosphomolybdic ($NbPMo_{12}Pyr$) and phosphovanadomolybdic acids, $NbPMo_{12}Pyr$ and $NbPMo_{11}VPyr$, respectively, were investigated as precursors to materials that catalyze the oxidative dehydrogenation of ethane to ethylene and acetic acid at atmospheric pressure. The effects of feed composition, steam flow, temperature, and precursor composition on catalytic activity and selectivity are presented for both ethane and ethylene oxidation. The productivity of ethylene and acetic acid from ethane using the catalytic materials formed from these precursors exceeds those reported in the literature for Mo–V–Nb–O_x systems under atmospheric or elevated pressure. Also, the production of acetic acid from ethylene is greater than that observed from Mo–V–Nb–O_x systems. Water is found to aid in desorption of acetic acid, thereby limiting deep oxidation to carbon oxides. Addition of vanadium reduces catalytic activity and selectivity to both ethylene and acetic acid, whereas niobium is essential for the formation of acetic acid from ethane. Other metals, such as titanium, tantalum, zirconium, antimony, iron, and gallium, do not provide the same beneficial effect as niobium. A balance of niobium and protonated pyridine in the catalyst precursor is required to produce an active catalyst by thermal treatment in nonoxidizing environments. Molybdenum and niobium are also necessary for the creation of the active site for ethane activation, and niobium is directly involved in the transformation of ethylene to acetic acid. A reaction scheme is proposed for the production of acetic acid from ethane over the catalytic materials.

Keywords: Ethane; Ethylene; Ethanol; Acetic acid; ODH; Reduced heteropolyanions; Molybdenum; Niobium

1. Introduction

Acetic acid is one of the world's most important chemical products. Its primary use is in the production of acetate esters that are further processed to films, textiles, paints, dyes, artificial fibers, and glues. In 1997, worldwide production of acetic acid was 5.4 million tons [1]. As evidenced from the recent major expansion of acetic acid production capacity in China, the demand for acetic acid continues to rise. The dominant manufacturing process for acetic acid, which uses an iodide-promoted rhodium catalyst to very efficiently carbonylate methanol, was pioneered by Monsanto in 1968 [2]. This process has several disadvantages, however. Although the growing use of iodide-promoted iridium and ruthenium catalysts partially alleviates the high cost associated with using the rhodium catalyst, the process requires very-high-purity carbon monoxide to avoid deactivation. The gas phase oxidation of ethylene to acetic acid over a palladium-based catalyst was recently reported by Showa Denko [1]. Ethylene, produced mainly by high-temperature dehydrogenation, is relatively expensive.

Thorsteinson and co-workers were able to selectively catalyze the production of ethylene from ethane over a mixed-metal oxide of molybdenum, vanadium, and niobium at atmospheric pressure and moderate temperatures [3]. It was later discovered that acetic acid could be synthesized in high yield directly from ethane over the same catalyst at 2.1 MPa [4]. Production of acetic acid from ethane at atmospheric pressure

* Corresponding author. Fax: +1 626 568 8743.
E-mail address: mdavis@cheme.caltech.edu (M.E. Davis).
[1] Current address: Oxo Technology, ExxonMobil, Baton Rouge, LA, USA.
[2] Current address: Department of Chemistry, Queen's University, 90 Queen's Crescent, Kingston, ON K7L3N6, Canada.

0021-9517/$ – see front matter
doi:10.1016/j.jcat.2005.10.010

has also been demonstrated [5]. Doping with palladium greatly increased acetic acid production at elevated pressure at the expense of ethylene production; this was explained by the consecutive reaction of ethylene over a palladium-based Wacker-like active center [6]. Other mixed oxide systems, such as VO_x [7], VPO [7], and Mo–V–Nb–Te–O_x [8,9], have also exhibited selective ethane oxidation catalysis. A more complete summary of catalysts capable of ethane oxidation to ethylene and acetic acid can be found elsewhere [10]. All reported mixed-metal oxide catalysts capable of producing acetic acid from ethane contain vanadium.

Heteropolyanions, with their easily manipulated acid and redox properties, are well suited for use in the study of alkane activation [11–19]. Indeed, heteropolyanions have received significant attention for selective alkane activation reactions [17,18,20–28], including the reaction of ethane to ethylene and acetic acid [24,25,29–33]. Ueda et al. showed that a pyridine-exchanged molybdovanadophosphate that was partially reduced during thermal treatment was active and selective for the oxidation of propane to acrylic and acetic acids [32]. Li and Ueda demonstrated that pyridine-exchanged phosphomolybdic acid could selectively oxidize isobutane to methacrylic acid and ethane to acetic acid [33]. Davis and co-workers investigated the use of niobium- and pyridine-exchanged phosphovanadomolybdic and phosphomolybdic acids for the selective oxidation of propane and *n*-butane [20–22]. This group also provided an example showing that these catalysts are active for the selective oxidation of ethane to ethylene and acetic acid [20]. In this paper, the reaction of ethane to ethylene and acetic acid over phosphovanadomolybdic and phosphomolybdic acids is studied in detail.

2. Experimental

2.1. Catalyst preparation

2.1.1. $M_xPMo_{12}Pyr$ ($M = Nb, Mo, V, Ti, Ta, Zr$)

The preparation of niobium- and pyridine-exchanged phosphomolybdic acids was adapted from methods presented by Holles et al. [20]. Phosphomolybdic acid ($H_3PMo_{12}O_{40}$) was obtained from Aldrich and used without further purification. Exchange with molybdenum, niobium, titanium, tantalum, and zirconium was performed in the oxalate form as described previously [20]. Exchange with vanadium was accomplished by substitution of a vanadyl oxalate (GFS Chemicals) solution (0.06 g vanadyl oxalate/g water) for niobium oxalate in the above procedures. Synthesized materials are abbreviated as $M_xPMo_{12}Pyr$, where M is the exchange metal and x denotes the ratio of the metal M to phosphorus (Keggin unit). $Nb_{0.6}PMo_{12}Pyr$ denotes niobium and pyridine exchanged $H_3PMo_{12}O_{40}$ with Nb/P = 0.6.

2.1.2. $Nb_xPMo_{11}VPyr$

Phosphovanadomolybdic acid ($H_4PMo_{11}VO_{40}$) was obtained from Pred Materials or synthesized according to the method described by Tsigdinos and Hallada [34]. Niobium exchange was performed by first transforming niobium pentachloride into niobium oxalate. Niobium pentachloride 5.00 g (Alfa Aesar; 99.999% packed under argon) was loaded into a three-necked round-bottomed flask in a nitrogen atmosphere glove box and transferred to a Schlenk line. Then 41.3 mL of water was added dropwise via an addition funnel with stirring. Hydrogen chloride vapors were neutralized with a sodium hydroxide bubbler. The solution was basified (pH = 12) by dropwise addition of 12.5 mL ammonium hydroxide (J.T. Baker; 28.0–30.0%). The white precipitate was dried by aspiration overnight and dissolved into a prepared solution of 4.60 g oxalic acid (Aldrich, 99+%) in 86.96 g of water until the precipitate was completely dissolved.

Aliquots of the resulting clear niobium oxalate solution were added dropwise to solutions of 1 g $PMo_{11}V$/1.5 g water and stirred for 2 h at room temperature. The solutions were then heated with stirring to 80 °C until all of the water was evaporated. The resulting green solids were pulverized and slurried in water (1 g solid/6 g water). A seven-fold molar excess of pyridine solution (0.1 g pyridine/1 g water) was added dropwise to form a light-green precipitate. The solutions were stirred for 2 h at room temperature before being dried at 80 °C. The materials are abbreviated as $M_xPMo_{11}VPyr$, similar to those prepared from $H_3PMo_{12}O_{40}$.

2.1.3. $PMMo_{11}Pyr$ ($M = Fe, Ga, Sb, Nb$)

Polyatom substitution of phosphomolybdic acid was performed according to known methods for the cations niobium, iron, and antimony [20,24,30,35]. Substitution with gallium was adapted from the procedures for iron and antimony, because both antimony and iron substitutions are performed with ions in oxidation state three. A solution of 5.0 g $H_3PMo_{12}O_{40}$ in 28 mL of water was basified to pH = 4.4 with lithium carbonate (Aldrich; 99+%) to form the lacunary Keggin structure $PMo_{11}O_{39}^{7-}$. Then 1 molar equivalent of iron(III) nitrate hydrate (Aldrich; 98%), gallium(III) nitrate hydrate (Aldrich; 99.9%), potassium antimonyl tartrate hemihydrate (Acros; 99%), or niobium oxalate (H.C. Starck; 20.5 wt% niobium) was quickly added. The solutions were then stirred at room temperature for 2 h before being filtered to remove any insoluble products. Pyridine (0.230 g) was added until a yellow precipitate (blue for antimony substitution) was formed. A large excess of pyridinium chloride (8–9 g) was then added to the solution to increase yield. The solids were separated by centrifugation and washed in three 100 mL aliquots of water.

2.1.4. $M_xP[Fe, Ga, Sb, Nb]Mo_{11}Pyr$ ($M = V, Nb, Sb$)

Polyatom substitution was performed as described above. However, before the addition of pyridine and pyridinium chloride, a solution of vanadyl oxalate (0.023 g/L g of water), niobium oxalate (0.065 g/L g of water), or potassium antimonyl tartrate hemihydrate (0.50 g/L g of water) was added to achieve the desired ratio of exchange metal to Keggin unit. The solution was stirred for 1 h at room temperature to achieve a cloudy green slurry. Pyridine and pyridinium chloride were then added as described above.

2.1.5. $Nb_{0.68}PW_{11}VPyr$

Synthesis of niobium-exchanged phosphotungstic acid was performed as described previously [15,36]. Sodium metavanadate (0.764 g; Fluka; 98%) was dissolved in 12.53 g of water to obtain a clear solution. The metavanadate solution was added to a clear solution of 0.887 g sodium hydrogen phosphate (Aldrich; anhydrous) dissolved in 12.50 g of water and acidified with 0.65 mL of sulfuric acid (J.T. Baker; 95–99%). The clear reddish-brown solution was stirred for 20 min at room temperature. After the dropwise addition of 22.690 g of sodium tungstate dihydrate (Aldrich; 99%) dissolved in 20.99 g of water over 50 min, the solution was acidified with sulfuric acid to pH 1.47 and refluxed for 2 h before being cooled to room temperature and extracted with ether. The orange-red lower phase was set aside. The middle phase was acidified with 100 mL of 50 vol% water–50 vol% sulfuric acid before being re-extracted with 200 mL of ether. The orange-red lower phase was set aside, and the middle phase was separated twice more with 100 mL of ether, retaining the orange-red bottom phases. The orange-red phases were combined, and residual ether was removed overnight by an air stream, followed by room-temperature vacuum treatment for 1 day. The yield was 16 g of light-orange solid. The structure was verified by X-ray diffraction, ^{31}P nuclear magnetic resonance in D_2O (major peak at −13.915 ppm of $PW_{11}VO_{40}$; very minor peaks at −13.407 and −14.292 ppm of $PW_{10}V_2O_{40}$ and $PW_{12}O_{40}$, respectively), and Fourier transform infrared spectroscopy [ν_{as}(P–O) 1069 and 1095 cm^{-1}, ν_{as}(W–O) 966 and ∼980 cm^{-1} shoulder, ν_{as}(W–O–W) 887 and 806 cm^{-1}]. Niobium and pyridine exchange were performed as described previously.

2.2. Reactivity studies

Experiments were performed in a BTRS Jr. single-pass vertical reactor system (Autoclave Engineers) with a 1/2-inch stainless steel reactor tube. Reactive flows consisted of an organic, either ethane (Matheson, 99.9%), ethylene (Matheson, 99.5%), or ethanol (Aaper Alcohol, 100%), mixed with oxygen (Air Liquide, 99.5%), 5% argon in helium (Air Liquide, 99.999%), and steam. Steam was fed as liquid water via a syringe pump and vaporized at 150 °C by a mixing assembly. When ethanol was used as the organic feed, it was pumped into the system with water. Empirical flow rates were 4:2:4:5 mL/min organic:oxygen:argon/helium:steam. Total pressure was atmospheric. Standard reaction temperature was 380 °C. The reactor cabinet and transfer lines were heated to 150 °C.

Ethane was oxidized over 0.6 g of catalyst sieved to 35–60 mesh and dispersed in 1 mL of silicon carbide (16 mesh; Abrasives Unlimited), resulting in a catalyst bed volume of 1.6 mL. Ethylene and ethanol were oxidized over 0.3 g of catalyst diluted to 0.8 mL with silicon carbide. Feeding reactive mixtures over a silicon carbide blank at reaction temperature produced no oxidation activity for butane, propane, ethane, ethane and ethylene, ethylene, or ethanol feeds. Blank conditions resulted in no measurable ethanol dehydration. Catalysts were activated in situ under 300 mL/min of helium by ramping from 30 to 420 °C over 5 h and holding at 420 °C for 8 h (ethylene, ethanol) or 10 h (ethane), followed by a 0.67-K/min ramp to the reaction temperature. Thermal treatment at 420 °C is required for the removal of pyridine and reduction of the catalyst precursor to its active state [21].

Reactive flows were equilibrated for 1 h off-line before being introduced to the catalyst bed and for 1 h over the catalyst bed before gas sampling. Gaseous products were analyzed by on-line gas chromatography–mass spectroscopy (Hewlett–Packard GCD Plus) equipped with a Plot-Q capillary column. Oxygenated products were trapped at −78 °C and analyzed offline by an Agilent high-performance liquid chromatograph equipped with a Prevail C18 5 μm 250-mm column using a mobile phase of 1% acetonitrile and 99% 25 mM potassium dihydrogen phosphate solution acidified to pH 2.5 by orthophosphoric acid. Products were detected by a ultraviolet–visible diode array detector at 210, 254, or 290 nm. Reactor reproducibility was established over a series of five distinct ethane oxidation catalysts prepared independently by three different persons. Standard deviation in conversion and space-time yield to ethylene or acetic acid was <1%. The standard deviation for selectivity data was <2%. Reactivity data were verified at least in duplicate, with most data points reproduced in triplicate or greater.

3. Results

3.1. Ethane oxidation

Previous studies have shown that both niobium and pyridine are required for the selective oxidation of propane and *n*-butane and that niobium- and pyridine-containing phosphomolybdic acids promote ethane oxidation [20,22]. The effects of catalyst precursor composition on ethane oxidation are shown in Table 1. Unlike previous studies with *n*-butane, the pyridine-exchanged PMo_{12} catalyst is not active for ethane oxidation. Only when niobium and pyridine are present together in the catalyst precursor is there significant activity toward ethane oxidation. The addition of vanadium to the catalyst significantly reduces catalyst activity and the space-time yield to ethylene and acetic acid.

Ethane oxidation results obtained from varying the transition metal cations and polyatoms of the heteropolyanion precursors are given in Table 2. The cations of Ta, Sb, Zr, and Ti do not exhibit the beneficial effect of niobium in the catalyst. Furthermore, none of these cations results in a catalyst with significant

Table 1
Ethane oxidation as a function of catalyst composition at 16:8:16:20 mL/min (ethane:oxygen:helium:steam), GHSV 2250 h^{-1}

Catalyst precursor	Conversion (%)		Selectivity (%)			STY[a]	
	C_2	O_2	CO_x	C_2H_4	Acetic	C_2H_4	Acetic
PMo_{12}	0.1	0.9	100	0	0	0	0
$Nb_{0.4}PMo_{12}$	0.3	0.9	39	52.8	8.2	0.002	3.0E–04
$PMo_{12}Pyr$	0.6	2.8	70	30.5	0	0.002	0
$Nb_{0.4}PMo_{12}Pyr$	17	71	66	28	6	0.049	0.015
$Nb_{0.4}PMo_{11}VPyr$	4.6	14	48	40	11	0.018	0.005

[a] STY is in mmol/(min g_{cat}).

Table 2
Comparison of ethane oxidation for catalysts with various transition metal exchange cations (M), M/P = 0.4, at 16:8:16:20 mL/min (ethane:oxygen:helium:steam), GHSV = 2250 h^{-1}

Catalyst precursor	Conversion (%)		Selectivity (%)			STY[a]	
						C_2H_4	Acetic
	C_2	O_2	CO_x	C_2H_4	Acetic		
$TaPMo_{12}Pyr$	0.1	0.4	88	9	3.6	1.1×10^{-4}	1.6E–05
$SbPMo_{11}VPyr$	0.6	1.0	11	86	3.2	0.012	4.5E–04
$ZrPMo_{12}Pyr$	0.2	0.6	35	63	1.9	0.001	3.8E–05
$TiPMo_{12}Pyr$	1.3	6.0	81	18	0.6	0.006	1.9E–04
$(VO)_{0.5}PMo_{11}FePyr$	0.9	3.3	43	24	33	0.002	3.2E–03
$(VO)_{0.5}PMo_{11}GaPyr$	0.4	1.5	0	0	100	–	4.6E–03
$NbPMo_{12}Pyr$	17	71	66	28	6	0.049	0.015
$Nb_{0.5}PMo_{11}FePyr$	18	67	69	25	6	0.044	9.9E–03
$Nb_{0.5}PMo_{11}GaPyr$	18	67	65	30	5	0.059	8.6E–03
$Nb_{0.5}PMo_{11}SbPyr$	9	29	53	40	8	0.034	6.4E–03

[a] STY is in mmol/(min g_{cat}).

Table 3
Ethane oxidation data for $Nb_xPMo_{11}VPyr$ at 16:8:16:20 mL/min (ethane:oxygen:helium:steam), GHSV = 2250 h^{-1}

Nb/P (x)	Conversion (%)		Selectivity (%)			STY[a]	
	C_2	O_2	CO_x	C_2H_4	Acetic	C_2H_4	Acetic
0.04	1.8	6	40	51	9	0.010	0.002
0.2	5.5	18	49	41	11	0.023	0.006
0.4	4.6	14	48	40	11	0.018	0.005
0.68	7.4	24	52	36	12	0.022	0.007
0.85	6.1	22	54	36	11	0.022	0.007
1	7.0	26	60	31	9	0.020	0.006

[a] STY is in mmol/(min g_{cat}).

activity toward ethane oxidation (maximum conversion of 1.3% ethane). These results are in contrast to findings of previous studies with *n*-butane where activity was reduced by only a factor of two with substitution of Nb for cations of Ti, Mo, Cr, Zr, or V [20]. Likewise, polyatom substitution with Fe, Ga, and Sb is not able to produce an active catalyst in the absence of Nb (Table 2).

Previous studies have shown that *n*-butane oxidation is sensitive to the Nb/P ratio [20]. Moreover, cation exchange of the phosphomolybdic acids partially replaces charge-balancing protons associated with the Keggin structure. Some of these protons will be used to protonate added pyridine to form pyridinium ions. Thus, by adjusting the amount of charge compensating ion, it should be possible to fix the acidity of the catalyst. The results of varying the Nb/P ratio of $Nb_xPMo_{12}Pyr$ and $Nb_xPMo_{11}VPyr$ are presented in Tables 3 and 4. The vanadium-containing catalysts give decreased activity toward ethane at all but the lowest niobium loadings. Selectivity to ethylene is slightly enhanced and selectivity to acetic acid is nearly identical, but the synthesis of both products is reduced when vanadium is present. Without vanadium substitution, conversion reaches a maximum of 17.0% at Nb/P = 0.4, but space-time yield is maximized at Nb/P = 0.6 (0.053 mmol/(min g_{cat}) ethylene and 0.015 mmol/(min g_{cat}) acetic acid); when vanadium is present, there is no clear maximum production of ethylene or acetic acid. Selectivity to overoxidation products CO_x is also maximized at Nb/P = 0.4 for the vanadium-free catalyst. When

Table 4
Ethane oxidation data for $Nb_xPMo_{12}Pyr$ at 16:8:16:20 mL/min (ethane:oxygen:helium:steam), GHSV = 2250 h^{-1}

Nb/P (x)	Conversion (%)		Selectivity (%)			STY[a]	
	C_2	O_2	CO_x	C_2H_4	Acetic	C_2H_4	Acetic
0	0.6	2.8	70	30.5	0	0.002	0
0.04	0.7	2	12	42	46	0.003	0.004
0.2	5.9	17	40	49	11	0.030	0.006
0.4	17.0	71	66	28	6	0.049	0.010
0.6	15.9	58	62	29	9	0.053	0.015
0.8	11.7	40	54	36	10	0.050	0.014
1	10.6	34	49	42	9	0.048	0.011
0.4[b]	4.7	12.1	30	62	8	0.033	0.004

[a] STY is in mmol/(min g_{cat}).
[b] Exchanged with pyridinium chloride rather than pyridine.

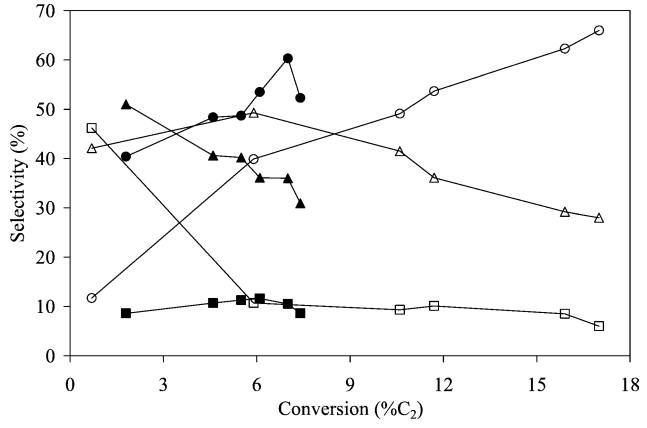

Fig. 1. Selectivity versus conversion for $Nb_xPMo_{11}VPyr$ (filled markers) and $Nb_xPMo_{12}Pyr$ (hollow markers); (●, ○) selectivity to CO_x, (▲, △) selectivity to ethylene, (■, □) selectivity to acetic acid.

pyridinium chloride is used instead of pyridine during catalyst synthesis, which should result in a more acidic catalyst, the activity of the catalyst is substantially reduced, whereas the selectivity to ethylene is substantially enhanced.

Fig. 1 presents an overlay of selectivity versus conversion data from the niobium-loading series experiments. Except for very low conversion ($Nb_xPMo_{12}Pyr$ series), the selectivity to ethylene decreases roughly linearly with increasing conversion, whereas the selectivity to deep oxidation products CO_x increases with increasing conversion for either catalyst series. The selectivity to acetic acid remains roughly constant. The samples in each series appear to lie more or less on a single selectivity-conversion curve. The vanadium-substituted catalysts exhibit higher selectivity to overoxidation products CO_x and lower selectivity to ethylene at the same level of conversion as the vanadium-free catalysts at all but very low conversions. It appears that substituting vanadium for molybdenum in the Keggin ion both inhibits catalytic activity and shifts the selectivity toward overoxidation products.

Reactivity data for the $Sb_xPMo_{11}NbPyr$ and $Nb_xPMo_{11}SbPyr$ series are presented in Table 5. At all but the lowest X/P (X = Sb, Nb) ratio, the selectivity profiles of either catalyst series are very similar, with carbon oxides and ethylene accounting for ∼50% and ∼45% at all values of X/P, respec-

Table 5
The effect of X/P ratio on ethane oxidation for catalysts containing Nb at 16:8:16:20 mL/min (ethane:oxygen:helium:steam), GHSV = 2250 h^{-1}

Catalyst precursor	Conversion (%)		Selectivity (%)			STY[a]	
	C_2	O_2	CO_x	C_2H_4	Acetic	C_2H_4	Acetic
$Nb_{0.15}PMo_{11}SbPyr$	5	16	47	45	8	0.024	4.3E–03
$Nb_{0.5}PMo_{11}SbPyr$	9	29	53	40	8	0.034	6.4E–03
$Nb_{1.0}PMo_{11}SbPyr$	2	6	49	49	2	0.011	4.0E–04
$Sb_{0.15}PMo_{11}NbPyr$	7	26	63	32	5	0.024	4.0E–03
$Sb_{0.5}PMo_{11}NbPyr$	7	24	53	43	5	0.031	3.5E–03
$Sb_{1.0}PMo_{11}NbPyr$	3	9	54	43	3	0.012	1.1E–03
$Nb_{0.40}PMo_{12}Pyr$	17	71	66	28	6	0.049	9.9E–03

[a] STY is in mmol/(min g_{cat}).

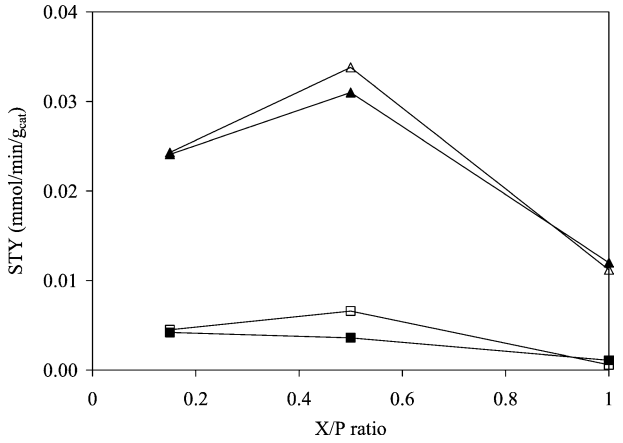

Fig. 2. Space-time yield of ethylene ((▲), X = Sb; (△) X = Nb) and acetic acid ((■) X = Sb; (□) X = Nb).

tively. The profile is easily visualized by plotting space-time yield as a function of X/P (Fig. 2). It appears that when niobium is present, the production of ethylene and acetic acid is a function of the X/P ratio rather than of the Nb/P ratio.

Numerous reports have highlighted the beneficial effect of steam on the oxidation of ethane to acetic acid [5–7,37,38]. These studies suggest the possibility of an optimal steam partial pressure for the oxidation of ethane. The effect of steam in the feed is shown by the data given in rows 1–4 of Table 6. Conversion is roughly constant up to a 20-mL/min steam feed. Selectivity to carbon oxides decreases as steam is increased, whereas selectivities to ethylene and acetic acid are enhanced. The production of both acetic acid and ethylene passes through a maximum at a 20-mL/min steam feed due to decreasing conversion. These trends are repeatable at either 2250 or 4500 h^{-1} (data not shown) gas hourly space velocity.

Comparing rows 3, 7, and 8 of Table 6 shows that the catalysts are most active in reducing environments (ethane:oxygen ratios of 2 and 5), but maintain high yields to ethylene and acetic acid even in mildly oxidizing environments (ethane:oxygen ratio of 0.5). This is consistent with previous studies for propane and *n*-butane oxidation [20]. Rows 9–11 in Table 6 demonstrate the result of decreasing the reaction temperature from 380 to 340 °C. As expected, conversion decreases with temperature, but selectivity to ethylene and acetic acid increases because of less overoxidation to carbon oxides. The space-time yield of ethylene is somewhat more sensitive to temperature than that of ethylene. Extrapolating the data presented in rows 3, 5, and 6 of Table 6 to zero contact time (Fig. 3), it is apparent that ethylene and carbon oxides are primary products (53 and 34% selectivity, respectively), whereas acetic acid is a minor product (7% selectivity).

3.2. Ethylene oxidation

Ethylene is one possible intermediate of selective ethane oxidation [4,39]. The results of varying Keggin ion composition with niobium, molybdenum, vanadium, and tungsten are given in Table 7. Consistent with results for propane and *n*-butane [20], the presence of niobium, pyridine, and a transition metal cation is required for significant catalytic activity and, in this case, production of acetic acid. When these conditions are met, both carbon and oxygen conversions are maximized (rows 6–11 in Table 7). Comparing catalysts containing pyridine species and transition metal cations reveals that molybdenum is re-

Table 6
Ethane oxidation under various conditions over $Nb_xPMo_{12}Pyr$

Nb/P	Flow[a] (mL/min)	GHSV (h^{-1})	*T* (°C)	Conversion (%)		Selectivity (%)			STY[b]	
				C_2	O_2	CO_x	C_2H_4	Acetic	C_2H_4	Acetic
0.6	16:8:31:**5**	2250	380	14	53	69	27	5	0.039	7.0E–3
0.6	16:8:26:**10**	2250	380	12	45	66	27	7	0.034	9.1E–3
0.6	16:8:16:**20**	2250	380	15	55	60	31	8	0.051	1.4E–2
0.6	16:8:6:**30**	2250	380	9	30	52	36	12	0.033	1.1E–2
0.6	16:8:16:20	**4500**[c]	380	6	21	54	40	6	0.058	8.9E–3
0.6	32:16:32:40	**9000**[c]	380	3	9	46	46	8	0.058	1.1E–2
0.6	**8:16**:16:20	2250	380	13	13	68	23	9	0.014	5.4E–3
0.6	**20:4**:16:20	2250	380	13	97	60	30	10	0.048	1.5E–2
0.4	16:8:16:20	2250	**380**	18	73	66	28	6	0.049	1.1E–2
0.4	16:8:16:20	2250	**360**	12	43	54	37	9	0.041	1.0E–2
0.4	16:8:16:20	2250	**340**	7	22	41	46	13	0.032	8.6E–3

[a] Ethane:oxygen:helium:steam.
[b] STY is in mmol/(min g_{cat}).
[c] 0.3 g catalyst instead of 0.6 g catalyst.

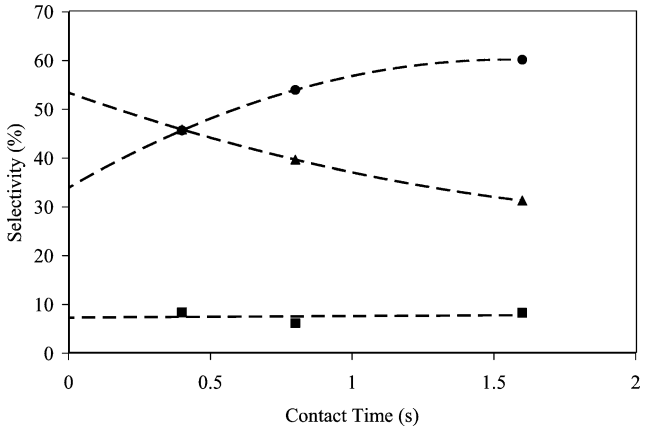

Fig. 3. Extrapolation of ethane oxidation data to zero contact time for $Nb_{0.6}PMo_{12}Pyr$ at 380 °C; (●) selectivity to CO_x, (▲) selectivity to ethylene, (■) selectivity to acetic acid.

Table 7
The effect of catalyst composition on ethylene oxidation at 16:8:16:20 mL/min (ethane:oxygen:helium:steam), GHSV = 2250 h^{-1}

Catalyst precursor	T (°C)	Conversion (%)		Selectivity (%)		STY[a]
		C_2	O_2	CO_x	Acetic	acetic
$PMo_{12}Pyr$	380	2	6	60	41	0.010
$PMo_{11}VPyr$	380	5	18	84	16	0.007
$PMo_{11}NbPyr$	380	5	19	71	29	0.014
$Mo_{0.68}PMo_{12}Pyr$	380	2	9	78	22	0.004
$(VO)_{0.68}PMo_{12}Pyr$	380	3	13	82	18	0.005
$Nb_{0.4}PMo_{12}Pyr$	380	31	100	75	21	0.059
$Nb_{0.68}PMo_{11}VPyr$	380	31	100	79	21	0.059
$(VO)_{0.50}PMo_{11}NbPyr$	380	27	100	79	21	0.058
	340	27	100	65	31	0.084
	300	27	96	53	44	0.123
$Nb_{0.68}PW_{11}VPyr$	380	4	22	97	3	0.001

[a] STY is in mmol/(min g_{cat}).

quired, but is insufficient on its own to affect significant reactivity (compare rows 4 and 11 with rows 6–8 of Table 7). Furthermore, niobium does not produce an active catalyst when molybdenum is not also present. Both niobium and molybdenum must be present for significant activity; the addition of vanadium does not affect reactivity. The catalysts produce a large and increasing amount of acetic acid as the temperature is lowered to 300 °C, because of decreased production of carbon oxides. Oxygen conversion remains nearly 100% even at 300 °C, whereas carbon conversion does not decrease. This indicates that further temperature reduction should reduce carbon oxides while maintaining high activity toward acetic acid. No ethanol was observed.

Because the amount of transition metal cation may affect the acidity of the catalyst, studies were conducted to determine whether an optimal Nb/P ratio exists for ethylene conversion. To obtain meaningful data, a space-time yield of 4500 h^{-1} and temperature of 300 °C were used. The resulting data, presented in Table 8, show a clear maximum in selectivity to acetic acid of 42% at Nb/P = 0.6, with carbon oxides minimized at 52% selectivity. Conversion rises with increasing Nb/P ratio, leading to a maximum space-time acetic acid yield of 0.16 mmol/(min g_{cat}) at Nb/P = 0.8. Acrylic

Table 8
Ethylene oxidation data for $Nb_xPMo_{12}Pyr$ at 16:8:16:20 mL/min (ethane:oxygen:helium:steam), GHSV = 4500 h^{-1} and 300 °C. AcA = acetic acid, Acr A = acrylic acid, MA = maleic acid

Nb/P	Conversion (%)		Selectivity (%)				STY[a]
	C_2H_4	O_2	CO_x	AcA	Acr A	MA	AcA
0.2	16	66	64	29	3.8	0.9	0.103
0.4	13	53	56	40	2.6	1.0	0.124
0.6	14	58	52	42	4.9	1.3	0.140
0.8	18	75	56	39	4.4	1.1	0.163
1	19	46	64	32	2.5	1.0	0.141

[a] STY is in mmol/(min g_{cat}).

Table 9
Effect of steam flow on ethylene oxidation at GHSV 4500 h^{-1} and 300 °C. AcA = acetic acid, Acr A = acrylic acid, MA = maleic acid

Flow (mL/min)	Conversion (%)		Selectivity (%)				STY[a]
	C_2H_4	O_2	CO_x	AcA	Acr A	MA	AcA
16:8:31:**5**	11	50	68	36	4.7	1.0	0.068
16:8:26:**10**	14	60	63	32	3.9	1.0	0.105
16:8:16:**20**	15	61	54	42	2.6	1.3	0.146
16:8:6:**30**	21	83	57	38	3.3	1.0	0.190

[a] STY is in mmol/(min g_{cat}).

acid production tends to decrease with increasing Nb/P ratio. Maleic acid is produced at a relatively constant low level of 0.002 mmol/(min g_{cat}), regardless of Nb/P ratio. Unlike Nb/P studies of ethane oxidation, selectivities to carbon oxides and acetic acid do not track with conversion.

The effect of steam flow on ethylene oxidation was also studied; results are given in Table 9. Carbon and oxygen conversions are increased with steam comprising up to 50% of the feed. The selectivity and production of acetic acid increase with steam feed, and the selectivity to carbon oxides tends to decrease with steam feed.

3.3. Ethanol oxidation

Selective oxidation of ethane to ethylene and acetic acid may occur through an adsorbed ethoxy intermediate [4,5]. However, ethanol is observed in only trace amounts during ethane oxidation at 200 °C and not at all during ethylene oxidation over $Nb_{0.4}PMo_{12}Pyr$ at 240 °C, most likely due to its high reactivity. Ethanol may be easily dehydrated to form ethylene and ether or may be partially oxidized to ethyl acetate, acetaldehyde, and acetic acid or fully oxidized to carbon oxides. The ability of the heteropolyanion system to catalyze these reactions was evaluated by increasing the temperature from 200 to 340 °C; the results are given in Table 10.

At temperatures below 300 °C, dehydration dominates, evidenced by the low oxygen conversion and the lack of significant amounts of acetic acid. Ethylene and ether are the major products. A dramatic shift in reaction profile occurs at 300 °C in which selectivity to acetic acid increases from 1 to 14%, ethanol conversion rises from 32 to 100%, and oxygen conversion is enhanced from 9 to 71%. Space-time yield to acetic acid increases by two orders of magnitude, from 0.007

Table 10
Ethanol oxidation over $Nb_{0.6}PMo_{12}Pyr$ at 16:8:16:20 mL/min (ethanol:oxygen:helium:steam), GHSV 4500 h^{-1}. AcetAl = acetaldehyde, EtOAc = ethyl acetate

T (°C)	Conversion (%)		Selectivity (%)						STY[a]	
	EtOH	O_2	CO_x	C_2H_4	Acetic	AcetAl	Ether	EtOAc	C_2H_4	Acetic
340	100	99	17	68	15	0	0	0	1.56	0.341
300	100	71	9	75	14	1	0	1	1.62	0.303
240	32	9	4	50	1	13	26	6	0.33	0.007
200	7	0	0	26	2	12	60	0	0.04	0.004

[a] STY is in mmol/(min g_{cat}).

Table 11
Ethanol oxidation as a function of catalyst composition at 16:8:16:20 mL/min (ethane:oxygen:helium:steam), GHSV = 4500 h^{-1} and 300 °C. AcetAl = acetaldehyde, EtOAc = ethyl acetate

Catalyst precursor	Conversion (%)		Selectivity (%)						STY[a]	
	EtOH	O_2	CO_x	C_2H_4	Acetic	AcetAl	Ether	EtOAc	C_2H_4	Acetic
$PMo_{12}Pyr$	100	9	1	89	1	9	–	–	2.06	0.028
$PMo_{11}VPyr$	73	17	2	52	2	24	17	3	0.89	0.042
$PMo_{11}NbPyr$	96	65	5	68	16	4	2	4	1.56	0.355
$Mo_{0.68}PMo_{12}Pyr$	98	9	1	88	1	8	1	–	1.88	0.029
$(VO)_{0.68}PMo_{12}Pyr$	86	11	–	67	2	20	9	1	1.15	0.038
$(Nb)_{0.68}PMo_{11}VPyr$	96	38	4	78	9	6	1	1	1.61	0.188
$Nb_{0.6}PMo_{12}Pyr$	100	71	9	75	14	1	–	1	1.62	0.303

[a] STY is in mmol/(min g_{cat}).

to 0.30 mmol/(min g_{cat}). At this temperature, ether production is eliminated, ethyl acetate production is decreased, and carbon oxide selectivity increases from 4 to 9%. At 340 °C, acetaldehyde and ethyl acetate production are completely eliminated, and both ethanol and oxygen conversion are 100%. Carbon oxides remain low, with a selectivity of 17%, whereas ethylene and acetic acid space-time yields remain high. Thus, unlike ethylene oxidation, ethanol oxidation is very selective to the partially oxidized products ethylene and acetic acid. Ethylene is preferred 5:1 over acetic acid.

The effects of varying catalyst precursor composition are presented in Table 11. In the presence of pyridine, both acid-exchanged and transition metal cation-exchanged forms of the catalysts show very high activity (>70%) toward ethanol, with ethylene as the major reaction product. However, addition of niobium in the acid form of the catalysts or within a transition metal cation-exchanged catalyst increases conversion to nearly 100%. In addition, only when niobium is present is oxidation to acetic acid appreciable at the expense of dehydration and other partially oxidized products, indicating that niobium may aid in the efficient oxidation process of the catalysts. Contrary to the results of ethane and ethylene oxidation, even the acid form of the catalyst ($PMo_{11}NbPyr$) is capable of selective oxidation and high conversion. In fact, space-time yield to acetic acid for this catalyst (0.36 mmol/(min g_{cat})) is greater than that for any other form of the catalyst examined. With or without niobium, the data given in Table 11 indicate that adding vanadium to the catalyst decreases ethanol conversion and enhances acetaldehyde and ether production at the expense of ethylene and acetic acid. Both carbon and oxygen conversions are decreased by the presence of vanadium. Thus, similar to ethane oxidation, the presence of vanadium is inhibitory to activity and selectivity.

4. Discussion

The performance of both $Nb_xPMo_{11}VPyr$ and $Nb_xPMo_{12}Pyr$ compares favorably to that of other ethane and ethylene oxidation catalysts reported in the literature (Table 12). Ethylene production is one order of magnitude greater than production of any other ethane oxidation catalyst at atmospheric pressure except Mo–V–Te–Nb oxide. However, other than $Nb_xPMo_{11}VPyr$ and $Nb_xPMo_{12}Pyr$, only VO_x/TiO_2 is able to produce acetic acid from ethane at atmospheric pressure. Both Mo–V–Nb and Mo–V–Nb–Pd oxides are able to catalyze the production of acetic acid from ethane at elevated pressure, but their space-time yield remains one order of magnitude below that of $Nb_xPMo_{11}VPyr$ and $Nb_xPMo_{12}Pyr$.

Both $Nb_xPMo_{11}VPyr$ and $Nb_xPMo_{12}Pyr$ are able to effectively oxidize ethane to acetic acid and ethylene at atmospheric pressure. These catalysts are also extremely active for the production of acetic acid from ethylene. Both activity toward ethane and selectivity to ethylene and acetic acid are enhanced when vanadium is absent from the catalysts. This result is unprecedented for ethane oxidation over molybdenum oxide catalysts. Usually, vanadium not only enhances selectivity to acetic acid, but also is required for significant activity [4–6,8,10,38]. This is most likely because vanadium is the active site for ethane activation in various molybdenum mixed-oxide systems [6–8,38,40], and in its absence, only ethylene can be produced [10,24,25,30]. Although vanadium has been identified as the active site for ethane oxidation in many molybdenum mixed-oxide systems, its role as an active site is not universally accepted for all systems. In the case of Mo–V–Nb mixed oxides, Mo^{5+} has been proposed as the activation and oxygen insertion center [3,4,41]. Furthermore, both V^{4+} and Mo^{5+} may be responsible for taking

Table 12
Comparison of ethane and ethylene oxidation catalysts. STY = space-time yield (mmol/(min g_{cat}))

Catalyst	Feed	T (°C)	P (atm)	Flow[a] (mL/min)	Conversion %C_2	Selectivity (%)		STY[b]		Reference
						C_2H_4	Acetic	C_2H_4	Acetic	
$Nb_{0.6}PMo_{12}Pyr$	C_2H_6	380	1	16:8:16:20	16	29	9	5.3E–02	1.5E–02	This work
	C_2H_4	340	1		26	–	29	–	1.8E–01	This work
$Nb_{0.68}PMo_{11}VPyr$	C_2H_6	380	1	16:8:16:20	7.4	36	12	2.2E–02	7E–03	This work
$Mo_{0.73}V_{0.18}Nb_{0.09}O_x$	C_2H_6	350	1	13.3:8.8:125.2:0	58	65	–	7.9E–03	–	[3]
			20	6:3.6:14.4:0	32	44	2.5	1.9E–02	1.1E–03	[10]
	C_2H_4	260	20	9:5:10:0	12	–	56	–	1.3E–02	[10]
$Mo_1V_{0.25}Nb_{0.12}Pd_{0.0005}O_x$	C_2H_6	246	14.8	11:2.2:12.4:1.8	4.7	19	62	3.8E–03	1.2E–02	[6]
	C_2H_4	247	5.2	2:24:40:40	99	–	93	–	1.0E–01	[6]
VO_x/TiO_2	C_2H_6	250	1	142:8.3:16.7:0	1	18	36	3.5E–03	6.9E–03	[7]
$Mo_1V_{0.39}Te_{0.16}Nb_{0.17}O_x$	C_2H_6	380	1	4.9:1.6:9.8	40	94	–	1.0E–01	–	[8]

[a] C_2:O_2:inert:steam quoted at standard temperature and pressure.
[b] STY is in mmol/(min g_{cat}) based on flow rates taken at standard temperature and pressure.

alkenes formed after initial activation on to their respective acids [5,42].

The presence of niobium is essential for efficient ethane activation to ethylene and acetic acid. Attempts to replace the niobium with V, Fe, Sb, Ga, Zr, Ti, and Ta did not result in active catalysts. When combined with niobium, Fe, Ga, and Sb were not able to improve catalytic performance. Previous studies have shown that the presence of niobium in molybdenum-based pyridine-exchanged heteropolyanion catalysts vastly improves the activity and productivity of *n*-butane oxidation to maleic acid and of propane oxidation to acrylic acid [20,22]. The beneficial effect of niobium has also been demonstrated in various other alkane oxidation systems [3,6,40–45]. The presence of niobium can improve the oxidation of light alkanes by modifying catalyst acidity [44], improving site isolation [41], affecting the distribution or redox centers [44], improving the stability of the active sites [4], and electronically promoting the active sites [45]. Although pyridine exchange of the heteropolyanion in the absence of niobium does allow for maleic acid and acrylic acid during butane and propane oxidation [20], respectively, ethane oxidation in the absence of niobium does not result in acetic acid, although small amounts of ethylene may be produced without niobium.

Although niobium is essential to ethane activity and acetic acid production, its beneficial effect is realized only when the catalyst precursor includes pyridine, niobium, and a transition metal cation (which may be niobium). Furthermore, the Nb/P ratio studies show a maximum conversion and acetic acid selectivity with Nb/P ratio and result in a roughly linear selectivity–conversion plot. When antimony is cation-exchanged in niobium-containing catalysts, the same trends are observed, although depressed by the presence of antimony. Taken together, these data suggest that although niobium is essential, the catalysts benefit from a balance of niobium and another factor related to the cation exchange (X/P) ratio.

Because the amount of cation exchanged adjusts the available protonation sites for added pyridine, one factor possibly related to the amount of cation exchange may be the acidity of the catalyst precursor and, subsequently, the activated material. Indeed, in Mo–V-based oxides synthesized in the presence of ammonia, the active site for propane oxidation is believed to be a combination of molybdenum and vanadium working in conjunction with a nearby acid site left behind during ammonia desorption [46]. When pyridinium chloride was used in place of pyridine during catalyst synthesis to produce a more acidic catalyst precursor, the resulting catalytic activity was similar to that of catalysts with low Nb/P ratios.

Niobium is required for significant oxidation of ethylene to acetic acid. Although some acetic acid can be formed from ethylene without the presence of niobium, adding niobium greatly improves the overall conversion and production of acetic acid. Furthermore, catalyst activity tends to increase with increasing niobium loading. Selectivity to acetic acid also increases with increasing niobium loading except for the very highest Nb/P ratios, where the catalyst's increased oxidizing ability results in overoxidation to carbon oxides. Niobium(IV), as determined by extended X-ray absorption fine structure experiments [21], thus appears to be directly involved in the transformation of ethylene to acetic acid. Other studies have shown that niobium alone is not sufficient to take ethylene on to acetic acid, although it is very capable of taking ethylene on to ethanol [47]. When tungsten was substituted for molybdenum, very little catalytic activity was observed, indicating that niobium is not able to elevate the activity of the tungsten-based material as it does for the molybdenum-based material.

The niobium- and pyridine-exchanged heteropolyanion system studied here can form maleic acid from propane through the oxidative dehydrogenation of propane to propylene followed by acid-catalyzed dimerization to C_6 branched hydrocarbons, precursors to maleic acid [48]. Thus, the formation of both acrylic acid and maleic acid from ethylene is not altogether surprising, perhaps the result of ethylene dimerization followed by further oxidation.

The results from ethylene oxidation, when correlated with the reduction potentials for heteropolyanion precursors reported by Song et al., show that the reduction potential of the cat-

alyst precursors is not correlated with catalytic activity [14]. This finding is not surprising, given that the incorporation of pyridine in the catalyst precursor provides a very powerful in situ reductant during thermal treatment, reducing 58% of the molybdenum from Mo^{6+} to Mo^{5+} and 100% of the niobium from Nb^{5+} to Nb^{4+} [21]. Thus small adjustments to reduction potential made by position and identity of transition metals in the catalysts are dominated by the reduced nature of the catalytic material after thermal desorption of the pyridine species. This allows the identity of the metal atoms to control the reactive properties of the catalytic materials.

Although water is required for the formation of acetic acid from ethane, it is also a product of ethylene production. During ethane oxidation over $Nb_{0.6}PMo_{12}Pyr$, increasing steam flow increased the selectivities of ethylene and acetic acid; however, activity passed through a maximum at 33% steam feed. A possible explanation for this effect is competitive adsorption of steam, ethane, ethylene, and acetic acid on the catalyst surface [6,7]. Similar studies performed during ethylene oxidation have shown that both activity and selectivity to acetic acid increase with increasing steam feed while carbon oxide production is decreased. This is consistent with previous results showing that water may aid the desorption of acetic acid from the surface of mixed-oxide catalysts, thus preventing further oxidation to carbon oxides [7,49].

Extrapolating the results of increasing space velocity during ethane oxidation to zero contact time produces carbon oxides and ethylene as the major products; however, a small (but nonzero) amount of acetic acid is also produced. The results of ethylene oxidation show that ethylene can also be oxidized to acetic acid in high yield. Thus, although the exact mechanism of reaction cannot be determined, the data suggest a reaction scheme as shown in Fig. 4. Ethane can be oxidized directly to ethylene and a small amount of acetic acid with large losses to carbon oxides. Ethylene is collected as a product or further oxidized to acetic acid with significant degradation to carbon oxides.

Besides the sequential pathway to acetic acid through initially formed ethylene, another possible route to ethylene and acetic acid involves an initial ethoxy intermediate yielding ethylene by β-elimination or acetic acid through α-elimination [4,5]. The 5:1 ratio of ethylene to acetic acid at zero contact time during ethane oxidation is nearly identical to the ratio of ethylene to acetic acid obtained during the efficient oxidation of ethanol, suggesting that an ethoxy intermediate may play a role in the production of ethylene and acetic acid from ethane in this system. Without the presence of niobium during ethanol oxidation, very little acetic acid is formed, but a significant amount of ethylene is produced. Thus, if an ethoxy intermediate is involved, there may be two sites competing for its conversion. One site, which does not require niobium, leads to ethylene. The other site, which requires the presence of niobium, produces acetic acid highly efficiently.

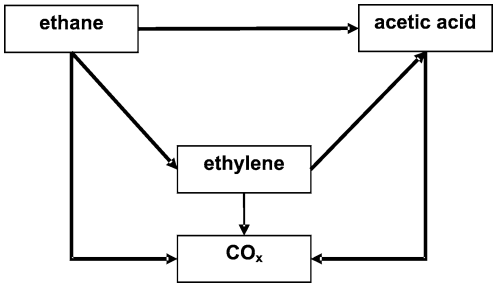

Fig. 4. Reaction scheme for the production of ethylene and acetic acid over partially reduced niobium exchanged phosphomolybdic Keggin type heteropolyanions.

5. Conclusion

Partial reduction of niobium- and pyridine-exchanged salts of phosphomolybdic and phosphovanadomolybdic acids at 420 °C forms solids that catalyze the oxidative dehydrogenation of ethane to ethylene and acetic acid at high yields at atmospheric pressure and moderate temperature under reducing conditions. The same catalysts also effectively convert ethylene to acetic acid at high yields under similar conditions. The production of acetic acid from ethane or ethylene over the catalytic materials at atmospheric pressure exceeds that reported in the literature for Mo–V–Nb–O_x systems at atmospheric or elevated pressure. Unlike other mixed-metal oxide systems reported in the literature, vanadium is not required for the formation of acetic acid from ethane. Vanadium-free catalysts are more active and selective than vanadium-containing catalysts. Niobium and pyridine are required for significant activity and for the production of acetic acid from ethane. Other metal cations, such as Ga, Fe, Sb, Zr, Ti, and Ta in either polyatom or exchange positions, are not able to replicate the function of niobium in ethane oxidation. The initial position of the niobium is relatively unimportant, but the balance of protonated pyridine and niobium present in the catalyst precursor affects catalytic activity and selectivity for the oxidation of ethane and ethylene.

Small variations in the reduction potential of the catalyst precursors do not correlate with catalytic activity of the activated materials, because partial reduction of the catalyst precursor during thermal treatment dominates the redox properties of the activated catalyst. The catalysts are most active and selective under reducing conditions, but are also very active under mildly oxidizing conditions. Adding steam to the reactive feed reduces ethane conversion but decreases carbon oxide production. Ethylene oxidation results demonstrate that adding steam to the feed increases the yield to acetic acid by aiding desorption of acetic acid from the catalyst surface, thereby preventing its further oxidation to carbon oxides.

Although the exact nature of the active site remains unknown, results show that ethane activation requires both niobium and molybdenum and a balance of another factor, possibly the catalyst acidity, affected by the transition metal cation exchange ratio. Niobium is directly involved in the conversion of ethylene to acetic acid and is required for significant production of acetic acid from ethanol. The data presented in this study implicate at least two pathways to acetic acid, a sequential pathway through initially formed ethylene and a simultaneous pathway through an initially formed ethoxy intermediate that is preferentially transformed to ethylene by β-H elimination.

Acknowledgments

This work was funded in part by BP-Amoco. J.M.G. acknowledges the support of a National Science Foundation graduate research fellowship.

References

[1] K.-I. Sano, H. Uchida, S. Wakabayashi, Catal. Surv. Jpn. 3 (1999) 55.
[2] G. Centi, in: G. Centi, F. Cavani, F. Trifiro (Eds.), Selective Oxidation by Heterogeneous Catalysis, Kluwer Academic/Plenum Publishers, New York, 2001, p. 514.
[3] E.M. Thorsteinson, T.P. Wilson, F.G. Young, P.H. Kasai, J. Catal. 52 (1978) 116.
[4] K. Ruth, R. Burch, R. Kieffer, J. Catal. 175 (1998) 27.
[5] M. Merzouki, B. Taouk, L. Monceaux, E. Bordes, P. Courtine, in: P. Ruiz, B. Delmon (Eds.), Studies in Surface Science and Catalysis, Proc. Third European Meeting on New Developments in Selective Oxidation by Heterogeneous Catalysis, Louvain-la-Neuve, Belgium, 8–10 April 1991, Elsevier, New York, 1992, p. 165.
[6] D. Linke, D. Wolf, M. Baerns, O. Timpe, R. Schlogl, S. Zeyß, U. Dingerdissen, J. Catal. 205 (2002) 16.
[7] L. Tessier, E. Bordes, M. Gubelmann-Bonneau, Catal. Today 24 (1995) 335.
[8] P. Botella, E. Garcia-Gonzalez, A. Dejoz, J.M.L. Nieto, M.I. Vazquez, J. Gonzalez-Calbet, J. Catal. 225 (2004) 428.
[9] J.M.L. Nieto, P. Botella, P. Concepcion, A. Dejoz, M.I. Vazquez, Catal. Today 91–92 (2004) 214.
[10] K. Ruth, R. Kieffer, R. Burch, J. Catal. 175 (1998) 16.
[11] S.Y. Yang, S.X. Xiao, T.L. Chen, R.S. Wang, Acta Chim. Sinica 58 (2000) 43.
[12] S.X. Xiao, S.Y. Yang, T.L. Chen, R.S. Wang, Huaxue Xuebao 59 (2001) 1165.
[13] D. Lapham, J.B. Moffat, Langmuir 7 (1991) 2273.
[14] I.K. Song, M.A. Barteau, J. Mol. Catal. A 212 (2004) 229.
[15] L. Ghizdavu, A. Fodor, G.S. Szasz, J. Therm. Anal. Calorim. 63 (2001) 907.
[16] M.S. Kaba, I.K. Song, M.A. Barteau, J. Vac. Sci. Technol. A 15 (1997) 1299.
[17] M. Langpape, J.-M.M. Millet, Appl. Catal. A 200 (2000) 89.
[18] N. Dimitratos, J.C. Vedrine, Appl. Catal. A 256 (2003) 251.
[19] C. Marchal-Roch, J.-M.M. Millet, Comptes Rendus de l'Académie des Sciences—Series IIC—Chemistry 4 (2001) 321.
[20] J.H. Holles, C.J. Dillon, J.A. Labinger, M.E. Davis, J. Catal. 218 (2003) 42.
[21] C.J. Dillon, J.H. Holles, R.J. Davis, J.A. Labinger, M.E. Davis, J. Catal. 218 (2003) 54.
[22] M.E. Davis, C.J. Dillon, J.H. Holles, J. Labinger, Angew. Chem. Int. Ed. 41 (2002) 858.
[23] J.H. Grate, J. Mol. Catal. A 114 (1996) 93.
[24] J.-S. Min, N. Mizuno, Catal. Today 66 (2001) 47.
[25] J.-S. Min, N. Mizuno, Catal. Today 71 (2001) 89.
[26] N. Mizuno, H. Yahiro, J. Phys. Chem. B 102 (1998) 437.
[27] F. Cavani, R. Mezzogori, A. Pigamo, F. Trifiro, Top. Catal. 23 (2003) 119.
[28] D. Casarini, G. Centi, P. Jiru, V. Lena, Z. Tvaruzkova, J. Catal. 143 (1993) 325.
[29] G.-P. Schindler, C. Knapp, T. Ui, K. Nagai, Top. Catal. 22 (2003) 117.
[30] S. Albonetti, F. Cavani, F. Trifiro, Catal. Lett. 30 (1995) 253.
[31] N. Haddad, C. Rabia, M.M. Bettaha, A. Barama, in: A. Corma, F.V. Melo, S. Mendioroz, J.L.G. Fierro (Eds.), Studies in Surface Science and Catalysis, Proc. 12th International Congress on Catalysis, Granada, Spain, 9–14 July 2000, Elsevier, New York, 2000, p. 1841.
[32] W. Ueda, W. Li, N.F. Chen, M. Kida, K. Oshihara, Res. Chem. Intermed. 26 (2000) 137.
[33] W. Li, W. Ueda, in: R.K. Grasselli, S.T. Oyama, A.M. Gaffney, J.E. Lyons (Eds.), Studies in Surface Science and Catalysis, Proc. 3rd World Congress on Oxidation Catalysis, San Diego, CA, 21–26 September 1997, Elsevier, New York, 1997, p. 433.
[34] G.A. Tsigdinos, C.J. Hallada, Inorg. Chem. 7 (1968) 437.
[35] J.-S. Min, M. Misono, A. Taguchi, N. Mizuno, Chem. Lett. 31 (2001) 28.
[36] M. Fournier, C. Feumi-Jantou, C. Rabia, G. Herve, S. Launay, J. Mater. Chem. 2 (1992) 971.
[37] D. Linke, D. Wolf, M. Baerns, S. Zeyß, U. Dingerdissen, J. Catal. 205 (2002) 32.
[38] M. Roy, H. Ponceblanc, J.C. Volta, Top. Catal. 11/12 (2000) 101.
[39] M.M. Bhasin, Top. Catal. 23 (2003) 145.
[40] P. Botella, J.M.L. Nieto, A. Dejoz, M.I. Vazquez, A. Martinez-Arias, Catal. Today 78 (2003) 507.
[41] R.K. Grasselli, J.D. Burrington, D.J. Buttrey, P.J. Desanto, C.G. Lugmair, A.F. Volpe, T. Weingand, Top. Catal. 23 (2003) 5.
[42] P. Botella, J.M.L. Nieto, B. Solsona, A. Mifsud, F. Marquez, J. Catal. 209 (2002) 445.
[43] R. Burch, R. Swarnakar, Appl. Catal. 70 (1991) 129.
[44] A.M.D.d. Farias, W.d.A. Gonzalez, P.G.P.d. Oliveira, J.-G. Eon, J.-M. Herrmann, M. Aouine, S. Loridant, J.C. Volta, J. Catal. 208 (2002) 238.
[45] B. Kilos, M. Aouine, I. Nowak, M. Ziolek, J.C. Volta, J. Catal. 224 (2004) 314.
[46] K. Oshihara, T. Hisano, W. Ueda, Top. Catal. 15 (2001) 153.
[47] K. Ogasawara, T. Iizuka, K. Tanabe, Chem. Lett. 15 (1984) 645.
[48] C.J. Dillon, J.H. Holles, M.E. Davis, J.A. Labinger, Catal. Today 81 (2003).
[49] J.L. Seoane, P. Boutry, R. Montarnal, J. Catal. 63 (1980) 191.